

High-performance bottom-contact devices based on an air-stable n -type organic semiconductor N , N -bis (4-trifluoromethoxybenzyl)-1,4,5,8-naphthalene-tetracarboxylic di-imide

Chia-Chun Kao, Pang Lin, Cheng-Chung Lee, Yi-Kai Wang, Jia-Chong Ho, and Yu-Yuan Shen

Citation: *Applied Physics Letters* **90**, 212101 (2007); doi: 10.1063/1.2741414

View online: <http://dx.doi.org/10.1063/1.2741414>

View Table of Contents: <http://scitation.aip.org/content/aip/journal/apl/90/21?ver=pdfcov>

Published by the [AIP Publishing](#)

Articles you may be interested in

[Air stable, ambipolar organic transistors and inverters based upon a heterojunction structure of pentacene on N , N -ditridecylperylene-3,4,9,10-tetracarboxylic di-imide](#)

Appl. Phys. Lett. **97**, 023506 (2010); 10.1063/1.3460282

[Efficient p - i - n type organic solar cells incorporating 1,4,5,8-naphthalenetetracarboxylic dianhydride as transparent electron transport material](#)

J. Appl. Phys. **104**, 034506 (2008); 10.1063/1.2963992

[Vertical structure p -type permeable metal-base organic transistors based on N , N -diphenyl- N , N -bis\(1-naphthylphenyl\)- 1 , 1 -biphenyl- 4 , 4 -diamine](#)

Appl. Phys. Lett. **92**, 232111 (2008); 10.1063/1.2944880

[Publisher's Note: "Air-stable n -channel organic thin-film transistors with high field-effect mobility based on N , N -bis\(heptafluorobutyl\)-3,4:9,10-perylene diimide" \[*Appl. Phys. Lett.* 91, 212107 \(2007\)\]](#)

Appl. Phys. Lett. **92**, 049902 (2008); 10.1063/1.2839368

[Air-stable n -channel organic thin-film transistors with high field-effect mobility based on N , N -bis\(heptafluorobutyl\)-3,4:9,10-perylene diimide](#)

Appl. Phys. Lett. **91**, 212107 (2007); 10.1063/1.2803073

The advertisement features a dark blue background with white and orange text. At the top left, it says 'NEW! Asylum Research MFP-3D Infinity™ AFM' in large white letters, followed by 'Unmatched Performance, Versatility and Support' in orange. On the right is the Oxford Instruments logo with the tagline 'The Business of Science®'. Below the text are four images: a blue textured surface, a brown textured surface, a grid of small yellow and red squares, and the MFP-3D Infinity AFM instrument itself. Text descriptions are placed around these images: 'Stunning high performance' next to the blue surface, 'Simpler than ever to GetStarted™' next to the brown surface, 'Comprehensive tools for nanomechanics' next to the grid, and 'Widest range of accessories for materials science and bioscience' next to the instrument.

High-performance bottom-contact devices based on an air-stable *n*-type organic semiconductor *N,N*-bis(4-trifluoromethoxybenzyl)-1,4,5,8-naphthalene-tetracarboxylic di-imide

Chia-Chun Kao and Pang Lin

Department of Materials Science and Engineering, National Chiao-Tung University, Hsinchu 300, Taiwan

Cheng-Chung Lee,^{a)} Yi-Kai Wang, Jia-Chong Ho, and Yu-Yuan Shen

Process Technology Division, Display Technology Center, Industrial Technology Research Institute, Hsinchu 310, Taiwan

(Received 29 March 2007; accepted 27 April 2007; published online 21 May 2007)

N,N-bis(4-trifluoromethoxybenzyl)-1,4,5,8-naphthalene-tetracarboxylic di-imide was applied to organic semiconductors for bottom-contact thin-film transistors. The carrier mobility was $1.6 \times 10^{-2} \text{ cm}^2 \text{ V}^{-1} \text{ s}^{-1}$, the threshold voltage (V_T) was +5.5 V, and the on/off current ratio was 8.6×10^5 . Devices without any further surface treatments were tested in an ambient environment. The threshold voltage shift (ΔV_T) was verified by gate bias stress measurements. A prototype compound, *N,N*-bis(4-trifluoromethylbenzyl)naphthalene-1,4,5,8-tetracarboxylic di-imide, shows direct correlation to the bottom-contact device with the varied molecular structure. © 2007 American Institute of Physics. [DOI: 10.1063/1.2741414]

Organic thin-film transistors (OTFTs) have wide applications in low-cost electronic devices such as flexible active displays, rf-ID tags, smart cards, and logic circuits.^{1,2} Many reports have illustrated the characteristics of OTFTs using pentacene, a well-known material, as the *p*-type organic transistor.³ In order to make complementary metal-oxide semiconductors more efficient, high-performance *n*-type organic transistors are needed. To date, several air-stable *n*-type materials have been studied.⁴⁻⁶ In particular, Katz *et al.* reported a series of *n*-type materials, namely, 1,4,5,8-naphthalene-tetracarboxylic di-imide (NTCDI), which were modified from 1,4,5,8-naphthalene-tetracarboxylic dianhydride using alkyl chain, benzyl, and phenyl structure.⁷ Although *n*-octyl-NTCDI has a high mobility, it cannot operate in air. The excellent electric properties and stabilization of 1*H*, 1*H*-perfluorooctyl-NTCDI and 4-trifluoromethyl-NTCDI were established with perfluorinated species. The perfluorinated group also provides resistance, protecting the molecular center from oxygen and moisture.

Most organic *n*-type devices are fabricated in a top-contact form.⁸ Dholakia *et al.* showed that bottom-contact devices show larger contact resistance than top-contact devices in some cases.⁹ In recent research, self-assembled monolayers (SAMs) were used as buffers to reduce heterogeneous electron transfers between the metal/dielectric and organic layers of the bottom-contact structure.¹⁰ Here, the source and drain electrodes were deposited beforehand on the dielectric layer, and then the organic layer was allowed to evaporate fully. Chemical reagents, including alkyl chains and terminal thionic groups, combined with the gold surface to form SAMs. The drawbacks of SAMs are that they only appear in particular chemical reactions, and the requisite gold electrodes increase the cost of making the transistors.

In this letter, we synthesize an organic *n*-type material, *N,N*-bis(4-trifluoromethoxybenzyl)-1,4,5,8-naphthalene-tetra-

carboxylic-di-imide (NTCDI-OCF₃) [Fig. 1(a)], and compare its electrical characteristics in a bottom-contact configuration with those of model compound *N,N*-bis(4-trifluoromethylbenzyl)naphthalene-1,4,5,8-tetracarboxylic di-imide (NTCDI-CF₃) [Fig. 1(b)]. The NTCDI-OCF₃ shows a mobility as high as $1.6 \times 10^{-2} \text{ cm}^2 \text{ V}^{-1} \text{ s}^{-1}$, which is higher than that of NTCDI-CF₃. Furthermore, all bottom-contact devices were fabricated without any surface treatments, and electric measurements were obtained in air. Table I compares the performance of both OTFTs.

The profile of the bottom-contact device is shown in Fig. 2. A layer of 100-nm-thick indium tin oxide (ITO) served as a bottom gate electrode. The gate dielectric layer was 300 nm thick and made of plasma-enhanced chemical vapor deposition silicon dioxide (SiO₂). For the top source and drain electrodes, ITO was sputtered on the top of the SiO₂. The defined channel length and channel width were, respectively, 30 and 500 μm. Finally, organic materials were thermally evaporated through a metal shadow mask in a high-vacuum chamber (pressure at 2×10^{-6} torr). While organic material evaporated, we maintained the optimum substrate temperatures: 40 °C for NTCDI-OCF₃ and 80 °C for NTCDI-CF₃. NTCDI-OCF₃ and NTCDI-CF₃ were prepared

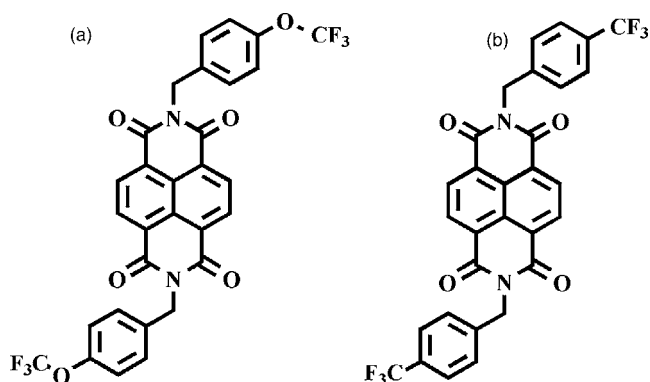


FIG. 1. Chemical structures of (a) NTCDI-OCF₃ and (b) NTCDI-CF₃.

^{a)} Author to whom correspondence should be addressed; electronic mail: leecc@itri.org.tw

TABLE I. Electrical characteristics of bottom-contact devices with the two semiconductors ($V_D = +50$ V).

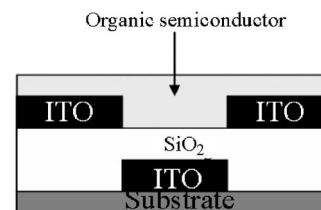
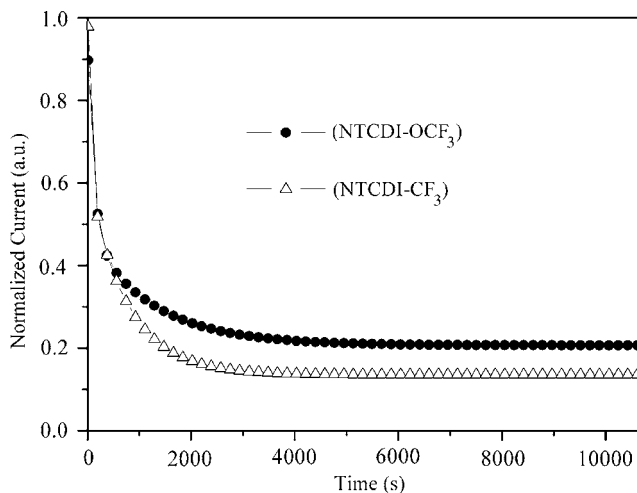
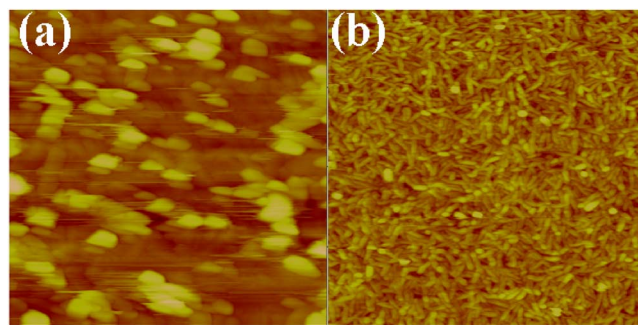
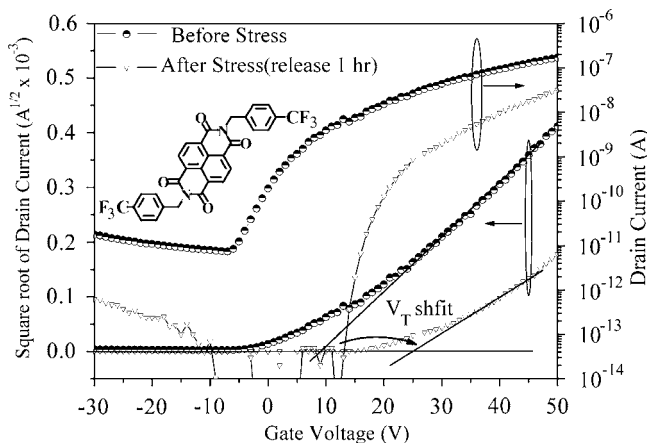
Semiconductor	Mobility ($\text{cm}^2 \text{V}^{-1} \text{s}^{-1}$)	On/off current ratio	Threshold voltage (V)
NTCDI- CF_3	9.7×10^{-4}	2.3×10^4	+11
NTCDI- OCF_3	1.6×10^{-2}	8.6×10^5	+5.5

according to well-established procedures.¹¹ Materials were purified at least twice sublimation which we use as the semiconductor layer.

As indicated in previous research, the mobility of top-contact devices made from NTCDI- CF_3 that use gold as the top electrode was $0.12 \text{ cm}^2 \text{V}^{-1} \text{s}^{-1}$. Our repetition of this test returned similar results: the calculated mobility was $0.1 \text{ cm}^2 \text{V}^{-1} \text{s}^{-1}$. We found that the performance of the OTFTs dropped off in the bottom-contact form. Although the NTCDI- OCF_3 top-contact device showed a slightly lower mobility than previously tested, $0.08 \text{ cm}^2 \text{V}^{-1} \text{s}^{-1}$, the transistor of the bottom-contact device showed excellent carrier mobility. Again, we must mention that no further surface treatments were placed on the top electrode or the dielectric layer of this bottom-contact device.

To understand how the bottom-contact devices performed when operated in a series, bias stress tests were performed (in a dark ambient environment). The device was operated with a continuing bias for 3 h and we measured the relative output current for each 5 s period. The biases of the gate voltage and drain voltage were set at a fixed value of +50 V, simulating real use of the transistor. The output current decay shown in Fig. 3 illustrates that NTCDI- OCF_3 maintained a significantly higher degree than NTCDI- CF_3 during the same bias period. Dholakia *et al.*, as mentioned above, demonstrated that bottom-contact devices have larger contact resistance than top-contact ones. The film growth of organic semiconductors appeared in varying stacking formations between the metal and oxide surfaces, resulting in imperfect molecule arrangements. The surface morphology of NTCDI- CF_3 and NTCDI- OCF_3 , as observed by atomic force microscopy (AFM) (Digital Instruments Nanoscope), is displayed in Figs. 4(a) and 4(b), respectively. As Fig. 4(b) clearly shows, NTCDI- OCF_3 has more continuous grain growth, which we believe to be suitable for a bottom-contact device. The NTCDI- OCF_3 bottom-contact device shows several advantages over NTCDI- CF_3 . It allows a further reduction in contact resistance, as well as less attrition of the current during series bias stress.

Gate bias stress may accompany a threshold voltage shift (V_T shift, ΔV_T) due to "charge trapping."¹² We measured the transfer characteristics, pristine state, and 1 h after the stress tests, using a semiconductor analyzer HP 4156A in an ambient environment. Results are shown in Figs. 5 and 6. The NTCDI- OCF_3 bottom-contact device showed less ΔV_T than NTCDI- CF_3 , and it maintained the almost the same electrical drain current performance and mobility after bias stress. In other research, no definite mechanism for bias stress has been studied.^{13,14} We focus on ΔV_T , which indicates the degree of the trapped charge and the long-term stability of the devices. The threshold voltage shifts of the transistors with NTCDI- CF_3 and NTCDI- OCF_3 are, respectively, +16 V (Fig. 5), and +7 V (Fig. 6). The NTCDI- OCF_3 bottom-

FIG. 2. Schematic diagram of bottom-contact device. $W/L=500/30 \mu\text{m}$.FIG. 3. Output current decay in NTCDI- OCF_3 (●) and NTCDI- CF_3 (Δ) OTFTs. Bottom-contact devices were stressed with a fixed voltage ($V_D = V_G = +50$ V) for a total of 3 h in air.FIG. 4. (Color online) AFM images ($5 \times 5 \mu\text{m}^2$) of NTCDI- CF_3 (a) and NTCDI- OCF_3 (b) were thermally deposited onto the SiO_2 surface.FIG. 5. Transfer curves show gate bias stress before and 1 h after: electrical characteristics of NTCDI- CF_3 .

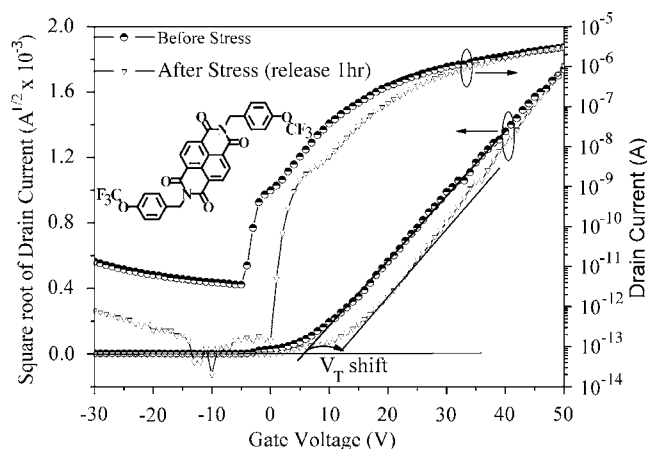


FIG. 6. Transfer curves show gate bias stress before and 1 h after: electrical characteristics of NTCDI-OCF₃.

contact device demonstrated superior stability under bias stress.

In conclusion, we have fabricated a bottom-contact device with a *n*-type organic semiconductor *N,N*-bis(4-trifluoromethoxybenzyl)-1,4,5,8-naphthalene-tetracarboxylic di-imide. The electrical characteristics of this device revealed a carrier mobility of $1.6 \times 10^{-2} \text{ cm}^2 \text{ V}^{-1} \text{ s}^{-1}$, threshold voltage of +5.5 V, and an on/off current ratio of 8.6×10^5 . A continuous arrangement of such molecule may reduce contact resistance and decay current. Our tests of the device under constant bias stress confirmed this. Furthermore, a

lower threshold voltage shift means that less charge trapping occurs after gate bias stress.

This work was supported by the Display Technology Center for the Industrial Technology Research Institute for Taiwan, R.O.C. (Contract No. 5461RE1110). The authors would like to thank L. H. Chan for helpful discussions.

- ¹C. D. Dimitrakopoulos and P. R. L. Malenfant, *Adv. Mater. (Weinheim, Ger.)* **14**, 99 (2002).
- ²B. Crone, A. Dodabalapur, Y. Y. Lin, R. W. Filas, Z. Bao, A. LaDuca, R. Sarpeshkar, H. E. Katz, and W. Li, *Nature (London)* **403**, 521 (2000).
- ³S. Iba, T. Sekitani, Y. Kato, T. Someya, H. Kawaguchi, M. Takamiya, T. Sakurai, and S. Takagi, *Appl. Phys. Lett.* **87**, 023509 (2005).
- ⁴H. E. Katz, A. J. Lovinger, J. Johnson, C. Kloc, T. Siegrist, W. Li, Y. Y. Lin, and A. Dodabalapur, *Nature (London)* **404**, 478 (2000).
- ⁵Z. A. Bao, A. J. Lovinger, and J. Brown, *J. Am. Chem. Soc.* **120**, 207 (1998).
- ⁶B. A. Jones, M. J. Ahrens, M. H. Yoon, A. Facchetti, T. J. Marks, and M. R. Wasielewski, *Angew. Chem., Int. Ed.* **43**, 6363 (2004).
- ⁷H. E. Katz, J. Johnson, A. J. Lovinger, and W. J. Li, *J. Am. Chem. Soc.* **122**, 7787 (2000).
- ⁸S. B. Heidenhain, Y. Sakamoto, T. Suzuki, A. Miura, H. Fujikawa, T. Mori, S. Tokito, and Y. Taga, *J. Am. Chem. Soc.* **122**, 10240 (2000).
- ⁹G. R. Dholakia, M. Meyyappan, A. Facchetti, and T. J. Marks, *Nano Lett.* **6**, 2447 (2006).
- ¹⁰B. Yoo, T. Jung, D. Basu, A. Dodabalapur, B. A. Jones, A. Facchetti, M. R. Wasielewski, and T. J. Marks, *Appl. Phys. Lett.* **88**, 082104 (2006).
- ¹¹A. Rademacher, S. Markle, and H. Langhals, *Chem. Ber.* **115**, 2927 (1982).
- ¹²D. Knipp, R. A. Street, A. Volkell, and J. Ho, *J. Appl. Phys.* **93**, 347 (2003).
- ¹³A. Salleo and R. A. Street, *J. Appl. Phys.* **94**, 471 (2003).
- ¹⁴M. Matters, D. M. de Leeuw, P. T. Herwig, and A. R. Brown, *Synth. Met.* **102**, 998 (1999).